Orion Service Module Reaction Control System Plume Impingement Analysis Using PLIMP/RAMP2

Xiao-Yen J. Wang
NASA Glenn Research Center, Cleveland, OH 44135

Forrest E. Lumpkin III
NASA Johnson Space Center, Houston, TX 77058

and

Frank Gati, James R. Yuko, and Brian J. Motil
NASA Glenn Research Center, Cleveland, OH 44135

The *Orion* Crew Exploration Vehicle Service Module Reaction Control System engine plume impingement was computed using the plume impingement program (PLIMP). PLIMP uses the plume solution from RAMP2, which is the refined version of the reacting and multiphase program (RAMP) code. The heating rate and pressure (force and moment) on surfaces or components of the Service Module were computed. The RAMP2 solution of the flow field inside the engine and the plume was compared with those computed using GASP, a computational fluid dynamics code, showing reasonable agreement. The computed heating rate and pressure using PLIMP were compared with the Reaction Control System plume model (RPM) solution and the plume impingement dynamics (PIDYN) solution. RPM uses the GASP-based plume solution, whereas PIDYN uses the SCARF plume solution. Three sets of the heating rate and pressure solutions agree well. Further thermal analysis on the avionic ring of the Service Module showed that thermal protection is necessary because of significant heating from the plume.

I.   Introduction

THE Orion project is under the Constellation program for the new space exploration vision initiated by President Bush in 2004. The Constellation program is responsible for providing the elements that will transport humans and cargo to both the International Space Station (ISS) and the Moon. These elements are the Crew Exploration Vehicle (CEV, or *Orion*), the Crew Launch Vehicle (Ares I), the Lunar Surface Access Module (Altair), and the Cargo Launch Vehicle (Ares V). *Orion*, with a crew of up to six astronauts, will launch on Ares I and then use its main engine to insert itself into a safe orbit to either dock with the ISS or with Altair. For the ISS mission, *Orion* will be responsible for separation, entry, descent, and landing. For the lunar missions, *Orion* also will have to maintain itself in low lunar orbit and perform the trans-Earth injection maneuver to return from the Moon. *Orion* consists of the Launch Abort System (LAS), Crew Module (CM), Service Module (SM), and Spacecraft Adapter (SA). The CM is a capsule design that provides the primary structure for crew support, incorporates the bulk of the avionics systems, and provides the capability for entry and parachute landing. The LAS will safely extract the CM from the launch configuration in the event of an early launch abort. The SM, the structure that interfaces with Ares I, will perform in-space flight propulsion operations and power generation.

Here, the SM was studied for its Reaction Control System (RCS) engine-plume-impingement effects. In a space environment, the exhaust plume of a rocket engine may expand so as to impinge upon the spacecraft structure or its components. Plume impingement will result in surface heating, pressure, and perhaps contamination. The SM RCS will operate in nearly all mission phases; the longest steady-state firing is 120 s. The SM radiator panel and solar arrays are the major concern and require a safe operational environment. Other surfaces or components might need thermal shields or protection from the plume impingement. Thrust loss is also a major concern for the guidance, navigation, and control of the vehicle.

The flow field inside the rocket engine and plume expansion into the ambient were computed using RAMP2, in which the flow is in two-dimensional or axisymmetric geometry with frozen or equilibrium chemistry. Boundary layer correction is also included in RAMP2 to account for viscous effects inside the nozzle. Details about the code are provided in Ref. 1.

The PLIMP code,[2] developed at the NASA Marshall Spaceflight Center, was used to compute the heating rate and pressure on the surfaces that are subject to plume impingement. Thus, the force and moment on the components are also available. In PLIMP, surfaces are represented using simple geometry surfaces, such as a cylinder, flat plate, or circular plate. The flow angle toward the surface and the flow regime, such as continuum, transitional, or free molecular, are considered in calculating the heating rate and pressure. Multiphase flows, such as solid particles and gases, can also be modeled. PLIMP can be used for general plume impingement analysis at both low and high altitudes.

The RPM code was used to predict the space shuttle orbiter Primary Reaction Control System plume impingement (forces and heating) on the ISS and other spacecraft near the shuttle orbiter. It uses a source flow assumption for the plume flow field where adjustable parameters in the formulation are set to achieve a best fit to a computational fluid dynamics (CFD) solution generated by the GASP code. The source flow assumption is generally accepted to be valid when the impingement distance is larger than 10 nozzle exit diameters. The source flow formulation in RPM divides the plume into inviscid and viscous regions in order to account for the boundary layer's affect on the plume. It uses the extended version of Simon's model in Ref. 3. Plume impingement forces and moments are determined by an engineering model that bridges between Newtonian and free-molecular analytic expressions for the pressure and shear coefficients. Plume impingement heating is also computed with an engineering model that bridges between continuum and free-molecular expressions for aerodynamic heating. This code was developed at the NASA Johnson Space Center and is described in Ref. 4.

The PIDYN code[*] uses a vacuum plume Newtonian approach for forces and moments, and basic heat-transfer calculation excerpts from MINIVER, the miniature version of the JA70 General Aerodynamic Heating Computer Code.[5] The SCARF code provides the plume flow field to PIDYN. SCARF also is based on Simon's model. In SCARF, the plume flow field is modeled much as in RPM by employing the source flow assumption and an adjustment for boundary layer expansion at an off-axis region. The primary difference between RPM and PIDYN is that the various adjustable parameters in PIDYN are based on characteristics of the engine (the most significant being the assumed ratio of specific heats), whereas in RPM the parameters are adjusted to match a CFD solution. This code was developed at Lockheed Martin and had heritage use at Lockheed Martin Space Systems for many spacecraft plume-impingement applications.

In summary, the RPM and PIDYN codes use a similar approach based on using a point source assumption to compute the plume field. However, the flow inside the engine nozzle changes dramatically from the nozzle throat to the exit, the plume solution will be sensitive to the specified ratio of the specific heat (γ) of the hot gas. The correct γ should be used for an accurate plume field. Both RPM and PIDYN codes can read in the mesh files generated by ProE for the geometries, which saves users from having to create the geometry from scratch. PLIMP will use a more accurate plume solution computed by RAMP2, but users will need to use an analytical approach and only structured mesh to define the geometry as a part of input to PLIMP. There is no interface between PLIMP and computer-aided design (CAD) software.

In the following sections, first the flow field inside the engine nozzle and its plume are presented; then the plume impingement results are presented for both forward-facing and after-facing thrusters, along with thermal analysis on the avionic ring of the SM. Finally, conclusions are drawn.

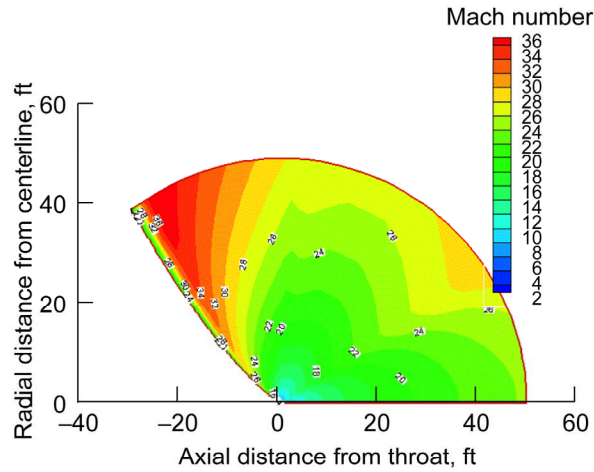[*]Castel, J. D., Private communication, Lockheed Martin, Denver, CO, June 2008.

II. Solution of the Flow Inside the Engine Nozzle and Its Plume

RAMP2 uses the chemical equilibrium compositions and applications (CEA) code to compute the thermodynamic and flow properties inside an engine nozzle. In Table 1, the CEA results of the pressure (P), temperature (T), density (ρ), molecular weight, specific heat (Cp), ratio of the specific heat (γ), sonic velocity, Mach number (Ma), and the mole fractions are listed for different locations inside the thruster. Given certain input parameters and CEA thermodynamic properties, RAMP2 can be used to compute the flow field inside the thruster and the plume. The contours of Ma, $\log_{10} \rho$, T, $\log_{10} p$, velocity (u), and flow angle are plotted in Fig. 1. At the throat, the gas could get as hot as 5000 °R, and at the nozzle exit, the temperature will reach approximately 900 °R. The plume will expand significantly because of the vacuum ambient.
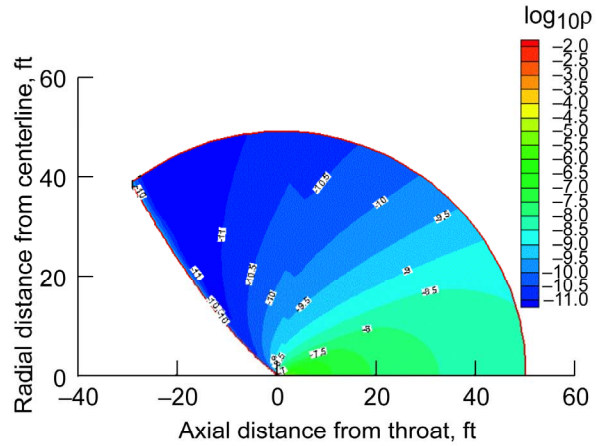
Figure 2 shows a comparison of the dynamic pressure ($1/2 \, \rho u^2$) between the RAMP2 and GASP solutions, and Fig. 3 shows a quantitative comparison along the axial direction at the circumferential angle (θ) = 0° and the circumferential direction at radius (R) = 15 ft. It can be seen that the RAMP2 plume solution agrees well with the GASP solution in the core of the plume; away from the core, the RAMP2 solution is generally higher than the GASP solution.

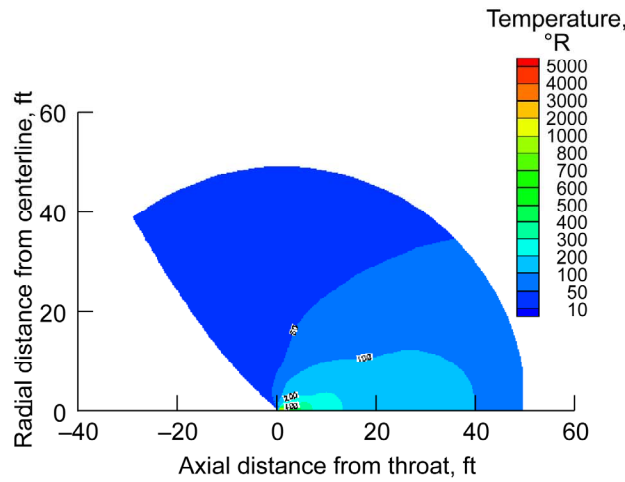**Table 1. Service Module Reaction Control System engine performance (CEA results)**

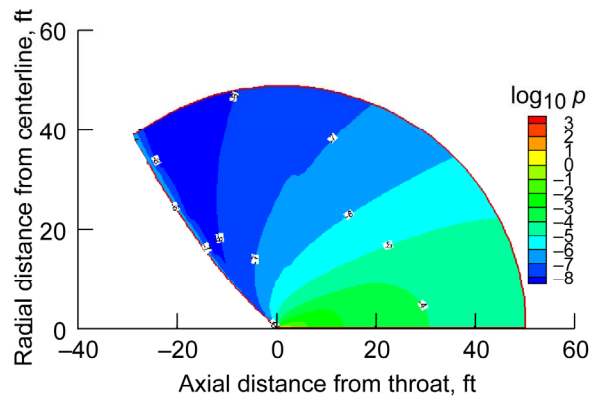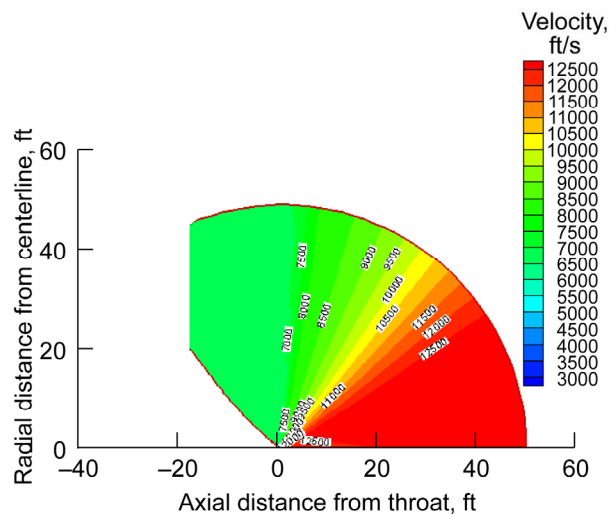|	Injector	Combustion chamber end	Throat	Nozzle exit
Pressure, P, bar	7.4463	7.2663	4.1986	0.00401
Temperature, T, K	3009.6	3004.33	2808.51	761.81
Density, ρ, kg/m^3	6.00×10^{-1}	5.86×10^{-1}	3.66×10^{-1}	1.31×10^{-3}
Molecular weight, 1/n	20.154	20.157	20.338	20.649
Specific heat, Cp, kJ/kg-K	4.4302	4.4228	3.7236	1.9971
Ratio of the specific heat, γ	1.157	1.157	1.1671	1.2528
Sonic velocity, m/s	1198.5	1197.4	1157.6	619.9
Mach number	0	0.146	1	5.225
Mole fraction				
CO	0.13447	0.13443	0.13334	0.03003
CO_2	0.03378	0.03384	0.03644	0.14234
H_2	0.16904	0.16904	0.17049	0.27943
H_2O	0.31516	0.31533	0.32534	0.2377
N_2	0.30201	0.30207	0.30528	0.31049

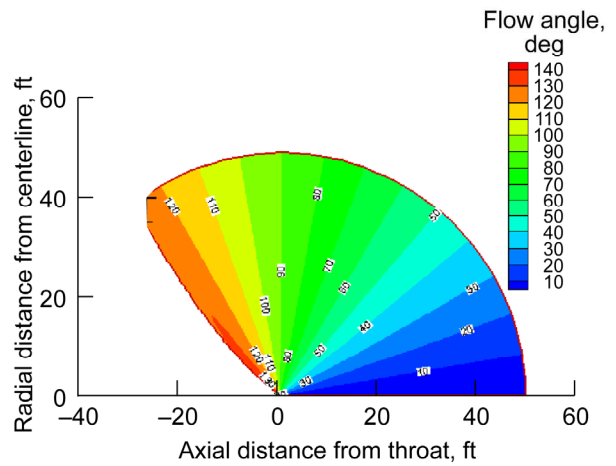(a) Mach number.

(b) $\log_{10} \rho$, lbm/ft^3.

(c) Temperature R.

(d) $\log_{10} p$, lbm/ft^3.

(e) Velocity, ft/s.

(f) Flow angle, deg.

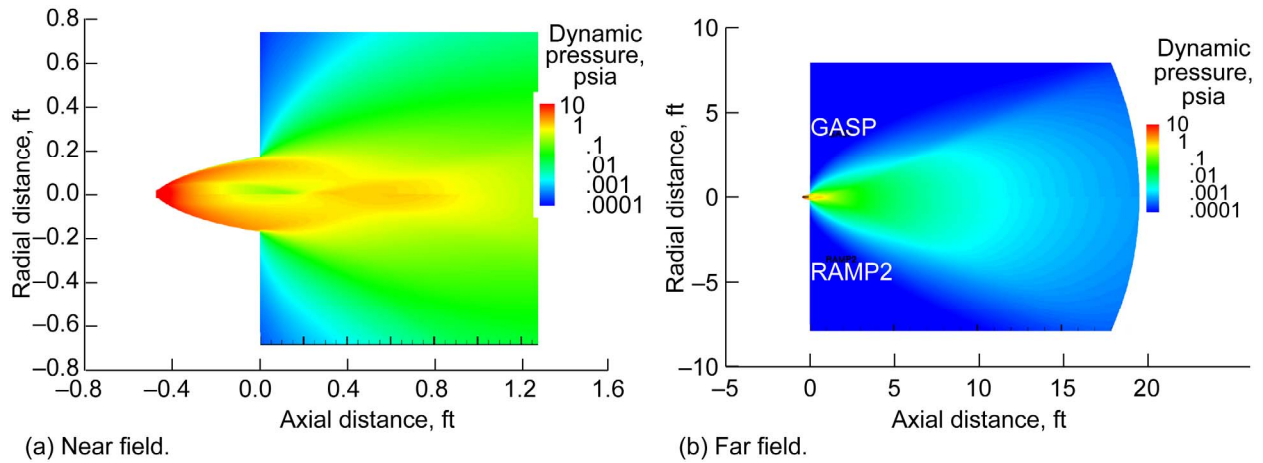**Figure 1. RAMP2 solutions of the flow inside the engine nozzle and its plume.**

(a) Near field.

(b) Far field.

Figure 2. Comparison of RAMP2 and GASP solutions of the flow inside the engine and plume.

(a) Dynamic presssure at $\theta = 0$.

(b) Dynamic presssure at $R = 14.96$ ft.

Figure 3. Comparison of RAMP2 and GASP solutions along the axial and circumferential directions.

III.   PLIMP Plume Impingement Results

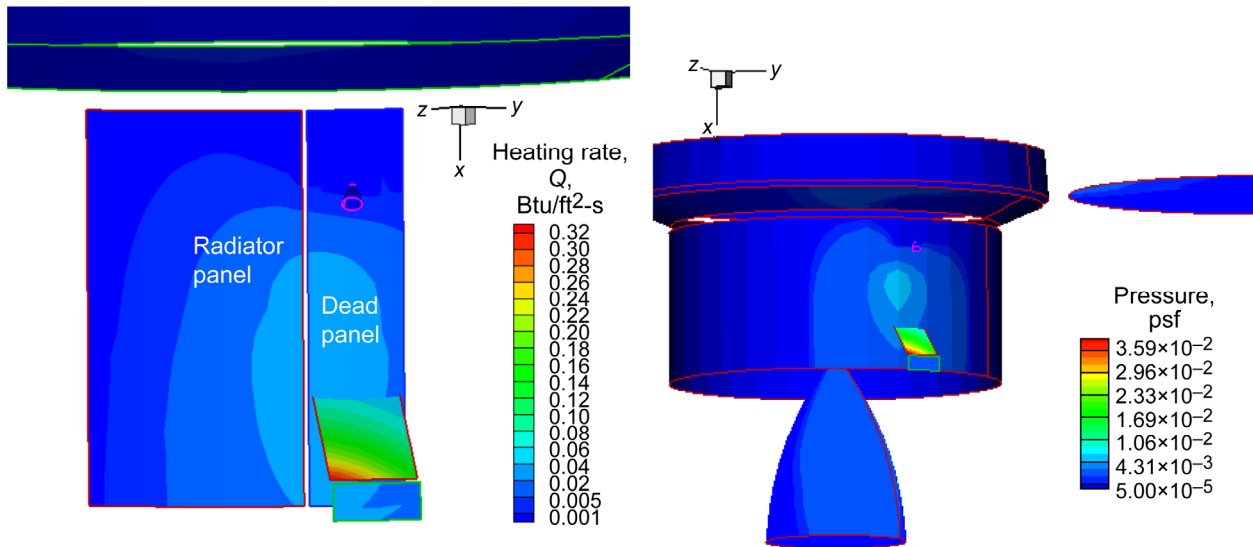Once the plume solution is available as an input to PLIMP, PLIMP can be run with additional input parameters, such as the definition of the impinging surfaces, the RCS engine location and orientation, and the surface wall temperature. Figure 4 shows plots of the contours of the heat flux and pressure on the SM for the aft-facing thruster with the assumption of a cold wall ($T_{wall} = 70$ °F). It shows that the dead panel underneath the RCS pod, the radiator panel, and the housing for auxiliary pod are subjected to plume impingement, where the flow is nearly transitional or free molecular. The maximum heating rate occurs on the housing of the auxiliary pod and reaches 0.35 Btu/ft^2-s. The heat flux on the radiator panel and the dead panel is not significant enough to cause any thermal concerns.

Figure 5 shows plots of the corresponding PLIMP results for the forward-facing thruster, showing that the worst spot is the avionic ring right next to the thruster, where the maximum heating rate could reach 7.4 Btu/ft^2-s. The flow around there is in the continuum flow regime and is turbulent. Since the heat flux is so significant, further thermal analysis was performed to compute the temperature to check whether any thermal protection or thermal shield is necessary for the avionic ring. The temperature results are presented in the following section.

Table 2 shows comparisons of the maximum heating rate and pressure among the PLIMP, RPM, and PIDYN solutions. The RPM and PIDYN solutions were explained in private communications.[*,†] The PLIMP solution agrees well with the RPM solution for both forward- and after-facing thrusters. The heating rate and normal force from PLIMP are expected to be higher than those from RPM since the RAMP2 solution is more conservative. The PIDYN heating rate and normal force on the avionic ring are lower than the PLIMP and RPM solutions for the forward-facing thruster, whereas the PIDYN solution agrees better with the PLIMP and RPM solutions for the after-facing thruster.

Table 2. Comparison of PLIMP, RPM, and PIDYN results
[T_{wall} = 70 °F.]

	PLIMP	RPM	PIDYN
Forward thruster (continuum flow)			
Maximum heating rate on avionic ring, Btu/ft^2-s	7.4	6.43	6.47
Maximum pressure on avionic ring, psf	11.3	13.1	5.99
Normal force on the avionic ring, lbf	3.7	3.6	2.81
Aft thruster(free molecule flow)			
Maximum heating rate, Btu/ft^2-s	0.35	0.178	0.287
Maximum pressure, psf	0.039	0.04	0.05

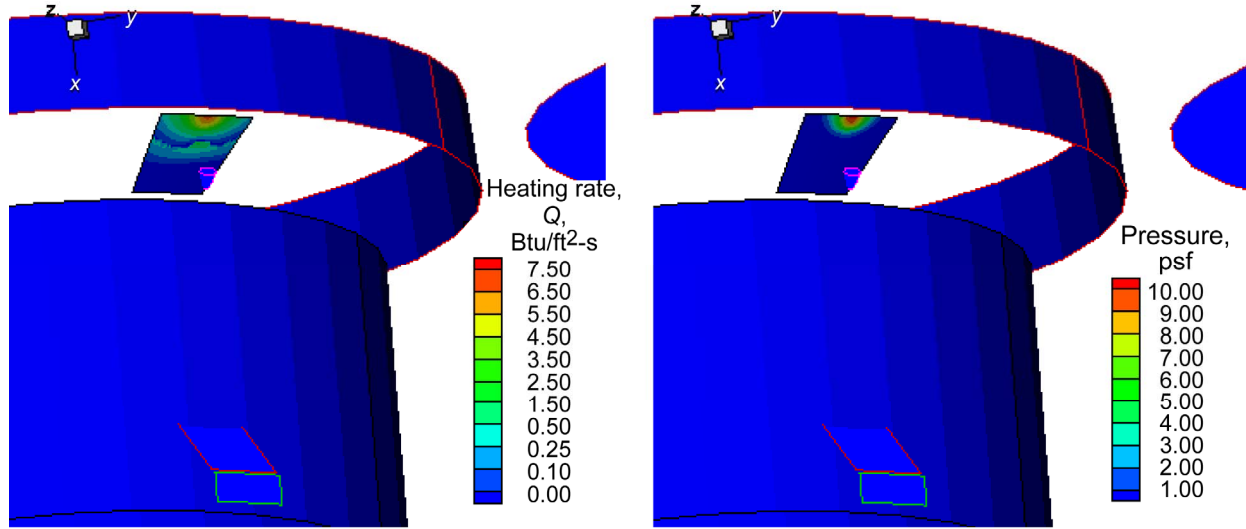**Figure 4. PLIMP results for the heating rate and pressure of the aft thruster.**

Figure 5. PLIMP results for the heating rate and pressure of the forward thruster.

IV.   Thermal Analysis on the Avionic Ring of the Service Module

On the avionic ring, the outer face sheet (OFS) and inner face sheet (IFS) are 0.035-in.-thick composite IM–7; in between is a 0.25-in.-thick aluminum honeycomb (H/C) core. In the thermal analysis, the plume impingement heating rate from PLIMP with T_{wall} = 294 K (70 °F) was imposed on the OFS; the contact resistance between the OFS and H/C core, and between the IFS and H/C core, was 11.3 W/m^2-K; the OFS radiated to deep space at T = 3 K with an emissivity of 0.88; and the IFS was adiabatic (insulated). The initial wall temperature was 3 K. There is a 3500-finite-element mesh in the MSC Patran/Pthermal model. The computed temperature contour at t = 120 s is plotted in Fig. 6, and the time history at the OFS, IFS, and H/C is plotted in Fig. 7. It can be seen that the temperature at OFS reaches 1260 °F within 40 s. Since the thermal resistance between OFS and H/C is high, not much heat goes through the H/C by conduction and most of the heat radiates to the ambient. Thermal protection or a thermal shield will be necessary for the area on the avionic ring that is subject to plume impingement since the temperature is far beyond the limit of the material.
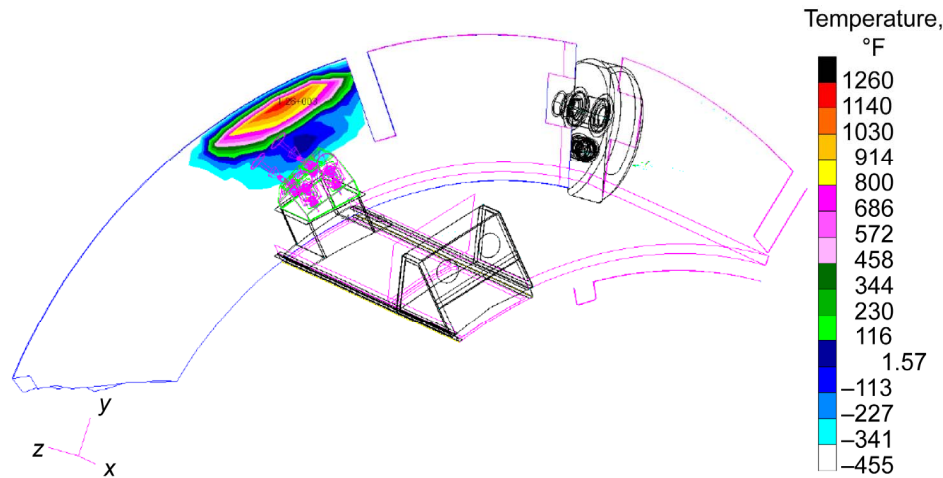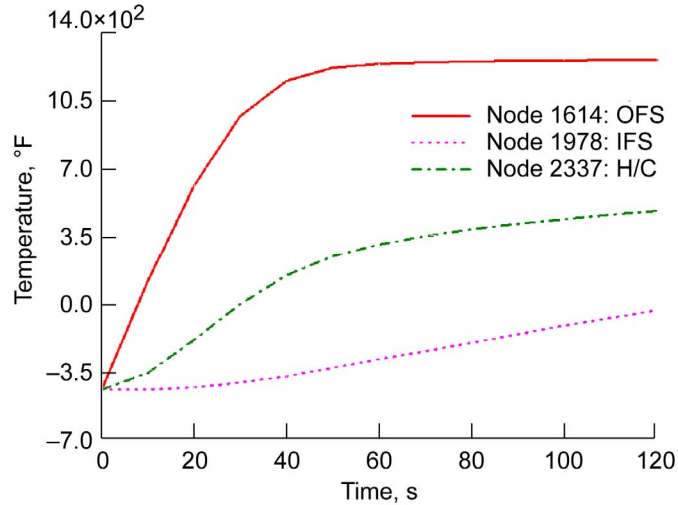

Figure 6. Temperature contour of the avionic ring at t = 120 s.

American Institute of Aeronautics and Astronautics

Figure 7. Temperature-time history of the outer face sheet (OFS), inner face sheet (IFS), and honeycomb (H/C).

V. Conclusions

Plume impingement of the *Orion* Service Module Reaction Control System was analyzed using the plume impingement program (PLIMP)/reacting and multiphase program 2 (RAMP2). The RAMP2 solution of the plume was compared with the GASP solution and showed good agreement. Furthermore, the PLIMP results, including heating rate and pressure (force) on the impinging surfaces were compared with the corresponding results from RPM and PIDYN. A reasonable agreement was achieved. Further thermal analysis on the geometry of most concern (avionic ring) on the Service Module showed that thermal protection or thermal shields are necessary.

Acknowledgments

References

1. Smith, S. D., "High Altitude Chemically Reacting Gas Particle Mixtures," LMSC–HREC TR D867400, Aug. 1984.
2. Wojciechowski, C. J., and Penny, M. M., "Development of High Altitude Plume Impingement Analysis for Calculating Heating Rates, Forces and Moments," LMSC–HREC D162867 I–III, Contract NAS8–25511, Mar. 1971.
3. Simons, G. A., "Effect of Nozzle Boundary Layers on Rocket Exhaust Plumes," *AIAA Journal*, Vol. 10, No. 11, 1972, pp. 1534, 1535.
4. Lumpkin, F. E., LeBeau, G. J., and Kanipe, D. B., "Model for Predicting Orbiter PRCS Plume Impingement Loads and Heating: RPM Ver. 3.1."
5. Wurster, K. E., "MINIVER—a Versatile Aerothermal Analysis/TPS Design Tool," Users Guide, Oct. 2000.